Korean Journal of Radiology

Evaluation of Left Atrial Appendage Isolation Using Cardiac MRI after Catheter Ablation of Atrial Fibrillation: Paradox of Appendage Reservoir

Hyungjoon Cho, MD[1], Yongwon Cho, PhD[1], Jaemin Shim, MD, PhD[2], Jong-il Choi, MD, PhD[2], Young-Hoon Kim, MD, PhD[2], Yu-Whan Oh, MD, PhD[1], Sung Ho Hwang, MD, PhD[1]

[1]Department of Radiology and [2]Division of Cardiology, Department of Internal Medicine, Korea University Anam Hospital, Seoul, Korea

Objective: To assess the effect of left atrial appendage (LAA) isolation on LAA emptying and left atrial (LA) function using cardiac MRI in patients who underwent successful catheter ablation of atrial fibrillation (AF).
Materials and Methods: This retrospective study included 84 patients (mean age, 59 ± 10 years; 67 males) who underwent cardiac MRI after successful catheter ablation of AF. According to the electrical activity of LAA after catheter ablation, patients showed either LAA isolation or LAA normal activity. The LAA emptying phase (LAA-EP, in the systolic phase [SP] or diastolic phase), LAA emptying flux (LAA-EF, mL/s), and LA ejection fraction (LAEF, %) were evaluated by cardiac MRI.
Results: Of the 84 patients, 61 (73%) and 23 (27%) patients showed LAA normal activity and LAA isolation, respectively. Incidence of LAA emptying in SP was significantly higher in LAA isolation (91% vs. 0%, $p < 0.001$) than in LAA normal activation. LAA-EF was significantly lower in LAA isolation (40.1 ± 16.2 mL/s vs. 80.2 ± 25.1 mL/s, $p < 0.001$) than in LAA normal activity. Furthermore, LAEF was significantly lower in LAA isolation (23.7% ± 11.2% vs. 31.1% ± 16.6%, $p = 0.04$) than in LAA normal activity. Multivariate analysis demonstrated that the LAA-EP was independent from LAEF ($p = 0.01$).
Conclusion: LAA emptying in SP may be a critical characteristic of LAA isolation, and it may adversely affect the LAEF after catheter ablation of AF.
Keywords: *Atrial fibrillation; Catheter ablation; Left atrium; Left atrial appendage; Magnetic resonance imaging*

INTRODUCTION

Atrial fibrillation (AF) is a common supraventricular arrhythmia, and it has been related to severe morbidity and mortality significantly in practice (1, 2). The AF-related arrhythmogenic substrate may be found in various cardiac structures such as the pulmonary vein, left atrium, or left atrial appendage (LAA) (1, 2). Recently, catheter ablation has been accepted as an effective treatment for AF because it helps in the electrical isolation of the arrhythmogenic substrates and terminates AF finally (2, 3).

LAA is an outpouching reservoir sac (4). Generally, the main transfer of accumulated blood from LAA to left atrium is defined as LAA emptying (4-6). Impairment of LAA emptying may cause blood stasis and thrombus formation in the LAA (4, 7). When performing catheter ablation for AF, the electrical isolation targets can include LAA and pulmonary veins (2, 8). LAA isolation by catheter ablation of AF may result in the impairment of LAA emptying, which may increase the risk of embolic stroke even after achieving sinus rhythm (2, 9). Therefore, the use of catheter ablation for LAA isolation has increased the need for monitoring the LAA hemodynamics in patients who underwent successful

catheter ablation of AF (2, 9).

Cardiac MRI can be useful in the evaluation of cardiac function and hemodynamics among patients with AF (10-13). Cardiac cine MRI consists of a movie loop at different cardiac time points, and it assesses the contraction and function of the cardiac chambers (11). Cardiac velocity encoding MRI (VENC-MRI) allows tracing of the velocity and direction of blood flow during a cardiac cycle (12, 14). To the best of our knowledge, no studies have been conducted on the use of cardiac MRI for LAA emptying after catheter ablation of AF.

Therefore, in this study, we aimed to evaluate the LAA emptying and left atrial (LA) function using cardiac MRI in patients who successfully terminated AF with catheter ablation, and to compare cardiac MRI measurements depending on the presence or absence of LAA isolation.

MATERIALS AND METHODS

Study Population

This retrospective study was approved by the Institutional Review Board of our hospital (2018AN0378), which waived the requirement for patients' informed consent due to the retrospective review of medical records and images. Through the Korea University Anam Hospital medical records system, we identified 415 patients (mean age, 55 ± 11 years [SD]; range, 31–76 years; 289 males [mean age, 55 ± 11 years; range, 31–76 years] and 126 females [mean age, 50 ± 11 years; range, 33–61 years]) who were referred for treatment of drug-refractory AF between June 2016 and May 2017. Inclusion criteria were follows: 1) catheter ablation of AF, 2) no recurrent AF for 12 months after catheter ablation, and 3) cardiac MRI for evaluation of heart function at 12 months following catheter ablation. Based on the inclusion criteria, 95 consecutive patients were retrospectively selected. Then, we excluded 11 patients because of 1) myocardial infarction (n = 4), 2) hypertrophic cardiomyopathy (n = 3), 3) mitral valve replacement status (n = 2), and 4) image artifacts of cardiac MRI (n = 2). Finally, a total of 84 patients (mean age, 59 ± 10 years; 67 males) who underwent cardiac MRI 12 months after the successful catheter ablation of AF were enrolled in this study (Fig. 1). The mean interval period between the cardiac MRI and catheter ablation of AF was 12 months (range, 11–14 months).

Catheter Ablation of AF

Catheter-based ablation of AF was performed using a

Between June 2016 and May 2017, patients visited for treatment of drug-refractory atrial fibrillation (AF) (n =415)

↓

Inclusion criteria
1. Catheter ablation of AF
2. No recurrent AF for 12-month follow-up
3. Cardiac MRI at 12-month follow-up

↓

95 consecutive patients were retrospectively selected.

↓

Exclusion conditions
1. Myocardial infarction (n = 4)
2. Hypertrophic cardiomyopathy (n = 3)
3. Mitral valve replacement status (n = 2)
4. Image artifact of cardiac MRI (n = 2)

↓

A total of 84 patients who underwent follow-up cardiac MRI after successful catheter ablation of AF

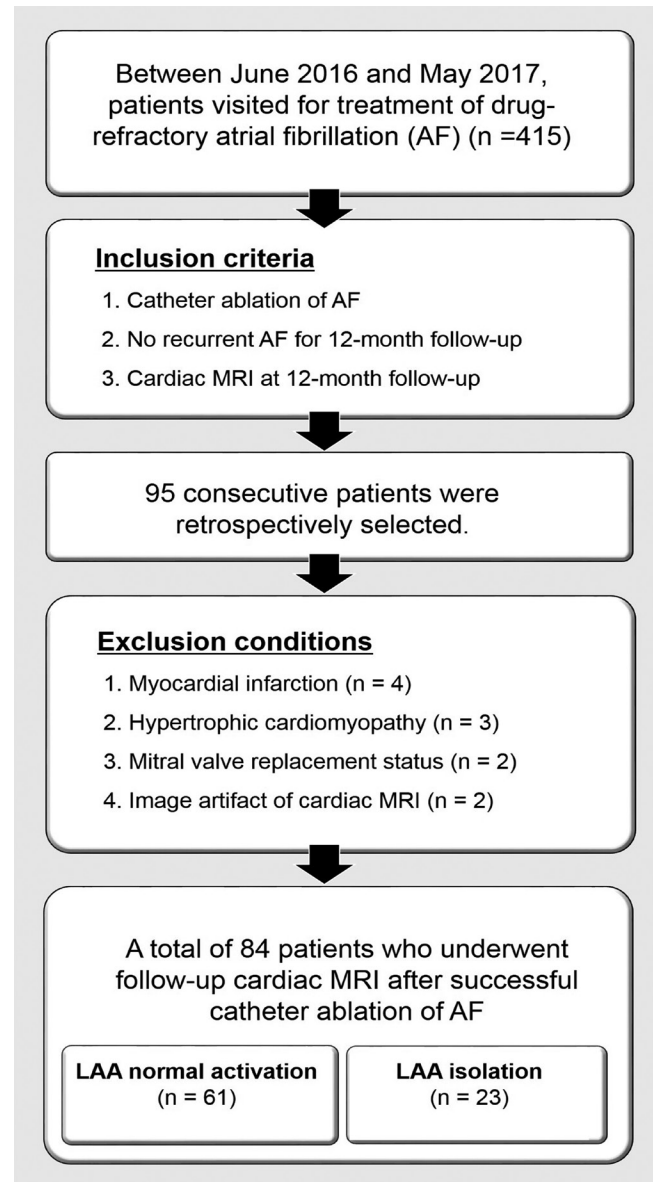| LAA normal activation (n = 61) | LAA isolation (n = 23) |

Fig. 1. Schematic diagram showing the selection of the study population. AF = atrial fibrillation, LAA = left atrial appendage

three-dimensional mapping (NavX, St Jude Medical Inc.) in all 84 patients. An intracardiac electrogram was recorded using a Prucka CardioLab™ Electrophysiology system (General Electric Medical Systems Inc.). For the electric isolation of arrhythmogenic substrates, radiofrequency energy was delivered through a Stockert generator (Biosense Webster Inc.) in a temperature-controlled mode and limited to 50°C using a maximal power of 35 W and duration of 30–40 seconds. In the routine catheter ablation of AF, the procedure endpoint was the complete electric isolation of the arrhythmogenic substrates such as the left atrium, LAA, and pulmonary veins.

Following sinus rhythm, LAA activation was evaluated using a catheter-based intracardiac electrogram. LAA activation was defined as the local "a" wave of LAA with or after the onset of the left ventricular QRS complex on the intracardiac electrogram (Fig. 2). Depending on the intracardiac electrogram results, all patients were divided into two groups: 1) LAA isolation (with the delay or absence of LAA activation) and 2) LAA normal activation (without the delay or absence of LAA activation).

Cardiac MRI Protocol

Cardiac MRI examinations were performed using a 3T MRI scanner (MAGNETOM Skyra, Siemens Healthineers) with a phased array 18-channel body matrix coil and 12-channel of the 32-channel spine matrix coil. The cardiac MRI protocol included cine, VENC, and late gadolinium enhancement (LGE) sequences. Electrocardiography (ECG)-gated cine MRI was performed in four- and two-chamber orientations of the left atrium using a steady-state free precession sequence. Cine MRI parameters were as follows:
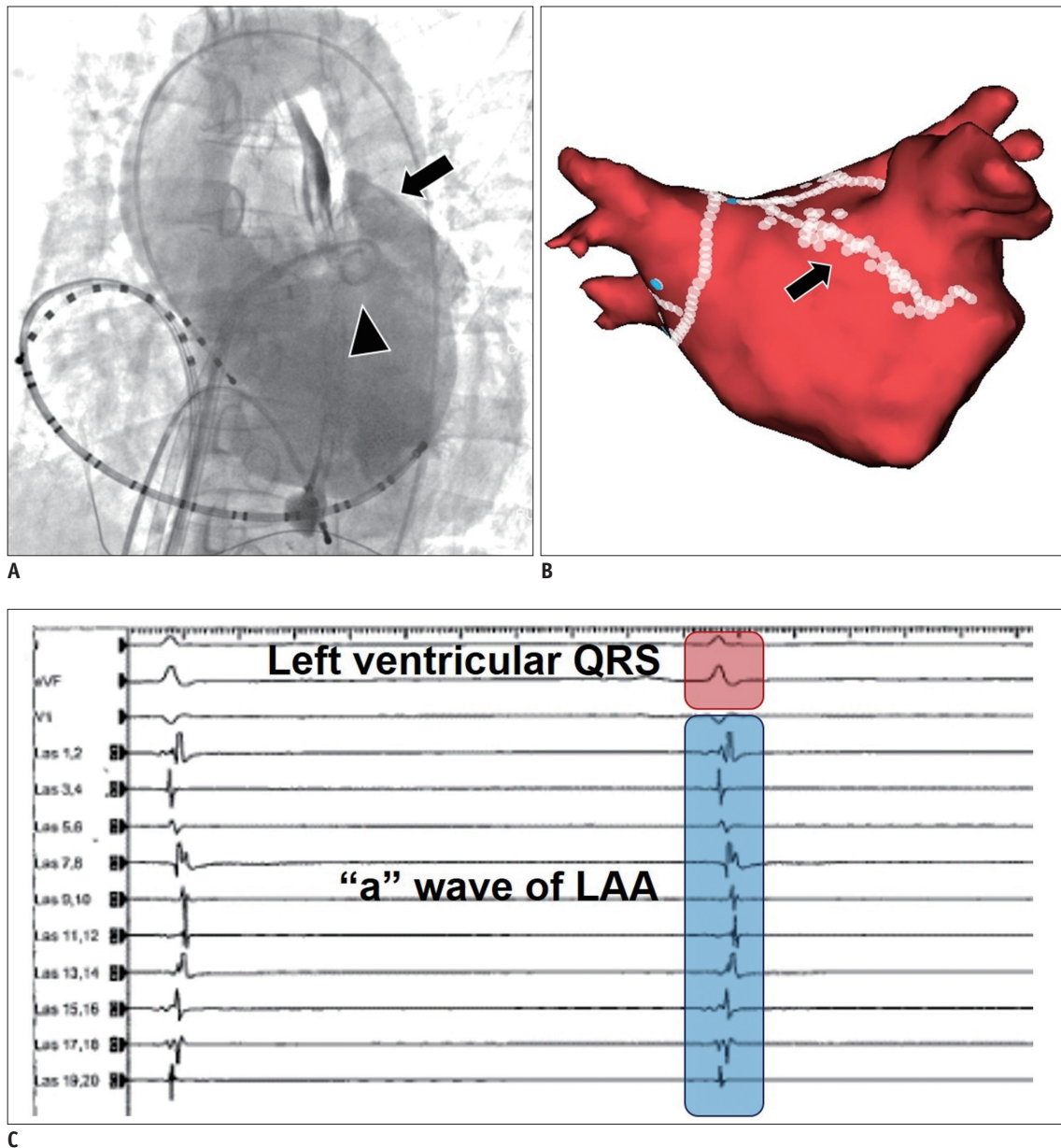

Fig. 2. Catheter ablation of AF and intracardiac electrogram.
Fluoroscopy **(A)** for catheter ablation of AF shows LAA (arrow) and ablation catheter (arrowhead). LA model **(B)** shows multiple dots which form ablation lines (arrow) for LAA isolation. Catheter-based-intracardiac electrogram **(C)** shows the local "a" wave of LAA (blue box) after the onset of the left ventricular QRS (red box). It is defined as LAA electrical isolation. LA = left atrial

field of view, 500 mm; slice thickness, 8.0 mm; voxel size, 2.0 x 2.0 x 8.0 mm; repetition time (TR)/echo time (TE), 240.4/1.0 msec; flip angle, 80°; number of cardiac phases, 25; and parallel acquisition technique (PAT) factor, 2. Then, a retrospective ECG-gated, two-dimensional flow-sensitive phase-contrast gradient-echo sequence was performed for VENC-MRI perpendicular to the LAA ostium. VENC-MRI parameters were as follows: TR/TE, 4.5/2.9 msec; flip angle, 15°; 30 frames per heartbeat; encoding velocity set, 200 cm/sec; PAT factor, 2. LGE-MRI data were acquired 15 minutes after intravenous injection of 0.2 mmol gadoterate meglumine (Dotarem, Guerbet) per kilogram of body weight using a three-dimensional inversion recovery gradient-echo pulse sequence with respiratory navigation and an ECG gating. A Look-Locker sequence with different inversion times was used to select the optimal nulling time for normal myocardium. LGE-MRI parameters were as follows: voxel size, 1.5 x 1.5 x 1.5 mm; TR/TE, 487/1.3 msec; flip angle, 15°; inversion time, 300–330 msec; and PAT factor, 2.

Cardiac MRI Analysis

All cardiac MRI data were analyzed independently by two radiologists using a commercial software workstation (TeraRecon iNtuition, TeraRecon).

LA function was evaluated based on the LA volume (LAV) determined with cine MRI. The reviewers assessed the LA areas on the perpendicular planes of the two- and four-chamber cine MRI. The LA axis length from the mitral annulus level to the posterior wall of the left atrium was also evaluated on the two-chamber cine MRI. The biplane area-length technique for the calculation of LAV was based on the following equation (6): LAV (mL) = (0.85 x LA area on the four-chamber cine MRI x LA area on the two-chamber MRI) / LA axis length on the two-chamber cine MRI. We calculated the maximum LAV (LAVmax) and minimal LAV (LAVmin) based on the LA areas and LA axis length determined with cine MRI, respectively (Fig. 3). In detail, the LAV and LA ejection fraction (LAEF) were as follows:

- LAVmin: LA end-diastolic volume at the first frame after mitral valve closure.
- LAVmax: LA end-systolic volume just before mitral valve opening.
- LAEF = (LAVmax - LAVmin) / LAVmax x 100.

LAA emptying flux (LAA-EF) and phase (LAA-EP) were evaluated with VENC-MRI. Reviewers traced the outer contours of the LAA ostium and descending aorta on VENC-MRI to evaluate both the LAA and aortic blood in a cardiac cycle (Fig. 3). Based on the VENC-MRI data, the maximum blood flux from the LAA to LA chamber was considered as LAA emptying. The maximum blood flux of LAA emptying was defined as LAA-EF (mL/s). If the LAA-EF was less than 35 mL/s, LAA emptying was defined as weak (15). Depending on the LAA and aorta blood flux curves, the LAA-EP was divided into: 1) LAA emptying in the diastolic phase (DP, LAA emptying combined with flattening of aortic blood flux simultaneously) and 2) LAA emptying in the systolic phase (SP, LAA emptying combined with a peak of aortic blood flux simultaneously) (Figs. 4, 5).

In LGE-MRI, LA ablation lines were distinguished from normal myocardium using an interactive tool for selecting intensity thresholds that correspond with LGE in the LA wall, as previously described (16). The percentile ratio of LA-LGE voxels to entire LA wall voxels was defined as the extent of LA-LGE. The LGE-MRI data were reformatted with a color look-up table mask for visualization of LA-LGE. Depending on the extent of LA-LGE, the LA-LGE after catheter ablation was classified into 3 grades: 1) mild (< 25% of LA wall), 2) moderate (≥ 25% and < 50% of LA wall, and 3) severe (≥ 50% of LA wall) (Fig. 3).

All cardiac MRI data analyses were repeated after an interval of at least 2 weeks. An additional reading was performed by the initial reviewers.

Statistical Analysis

All continuous data are presented as means ± SD, and all categorical data are expressed as absolute values and percentages. Intra- and interobserver reproducibility of cardiac MRI measurements was assessed using the intraclass correlation coefficient. An intraclass correlation coefficient of ≥ 0.7 was considered as statistically reproducible (17). K statistics was used to assess the intra- and interobserver agreement for weak LAA emptying and LAA-EP. The strength of the agreement was interpreted as follows: k-values of 0.61–1.00 indicated good agreement (18). Differences in variables between two different groups were evaluated using the Student's t tests and chi-square test, if appropriate. The Pearson correlation coefficient was used to evaluate the relationship between the LAVmin, LAVmax and LAA-EF depending on the LAA-EP. Univariate and multiple regression analyses were performed to determine the factors responsible for the difference in LAEF. In multiple regression analysis, a forward selection mode was used. The removal of variables was based on likelihood ratio statistics with a probability of 0.1. Eventually, the residual variables with
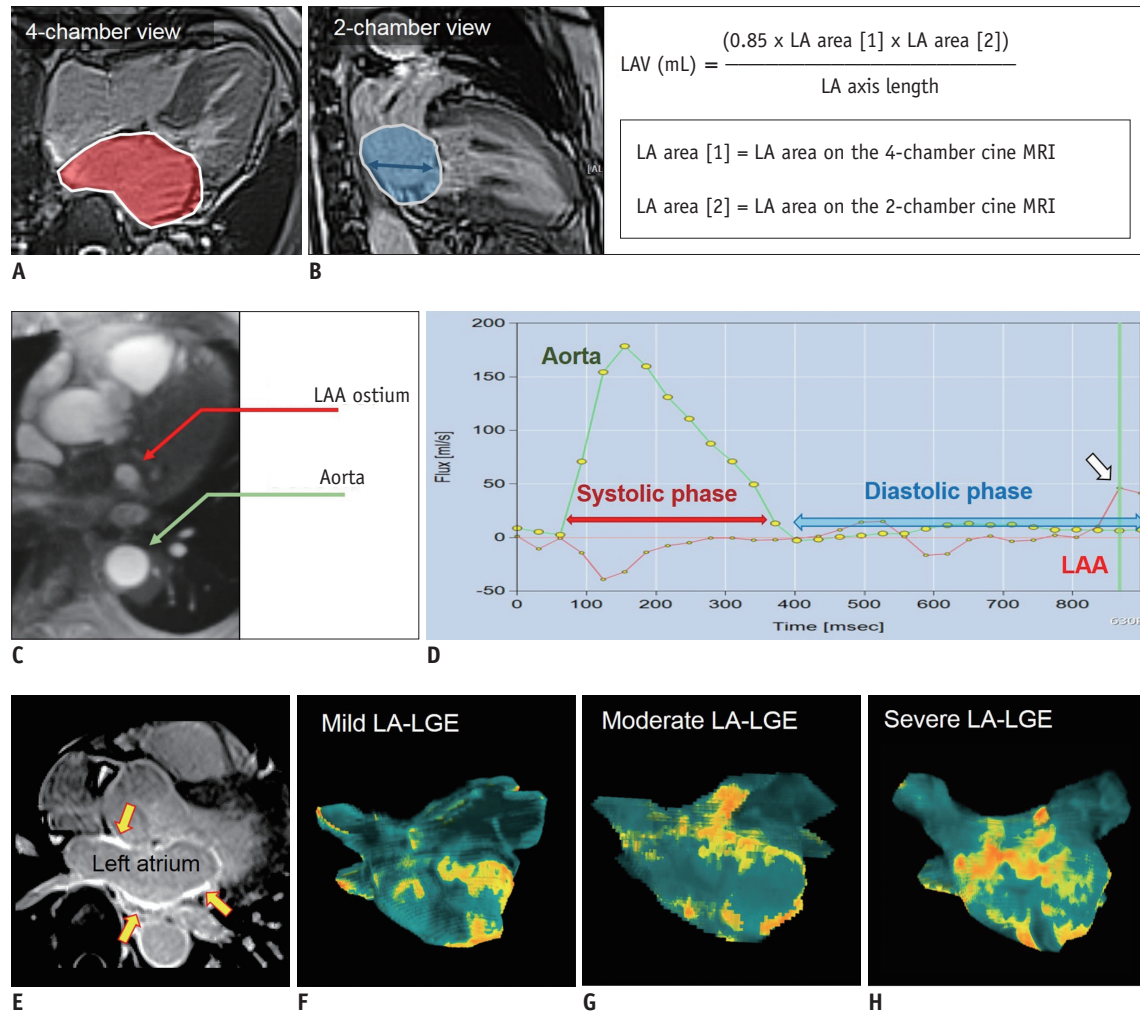
Fig. 3. Analysis of cardiac MRI.
Four-chamber **(A)** and two-chamber views **(B)** of cine MRI show two different LA areas and LA axis length for LAV. VENC-MRI **(C)** allows the measurement of blood flux in the LAA ostium and descending aorta. The graph **(D)** shows the changes in blood flux in a cardiac cycle. The blood flux of the aorta differentiates between the systolic and DP. Furthermore, the blood flux of LAA shows its peak value as LAA emptying (arrow) in the late DP. LGE MRI **(E)** shows thick LA walls of contrast enhancement (arrows) indicating the ablation lines. Three-dimensional LGE images **(F-H)** show three different grades of LA-LGE (yellow and red). DP = diastolic phase, LAV = LA volume, LGE = late gadolinium enhancement, VENC-MRI = velocity encoding MRI

p value of < 0.05 were considered independently related to the LAEF.

Statistical analysis was performed using the MedCalc Statistical Software Version 19.1.5 (MedCalc Software Ltd.; https://www.medcalc.org; 2020). A p value of < 0.05 was considered statistically significant.

RESULTS

Patient demographics are summarized in Table 1. Among all 84 patients, 61 (73%) and 23 (27%) patients had an LAA normal activation and an LAA isolation after catheter ablation, respectively. Clinical characteristics (e.g.,

age, sex, body surface area, hypertension, and diabetes mellitus) had no significant difference between the LAA normal activation and LAA isolation. In the AF types, the proportion of persistent AF was significantly greater in LAA isolation (15/23 [65%] vs. 22/61 [36%], $p = 0.01$) than in LAA normal activation.

In all 84 cardiac MRIs, quantitative MRI measurements were reproducible, and all the reviewers were in agreement for a weak LAA emptying and LAA-EP (Table 2). In comparison to the LA function (Table 3), LAA normal activation showed significantly lower LAVmin (29.7 ± 12.0 mL vs. 43.3 ± 10.7 mL, $p < 0.001$) and LAVmax (43.8 ± 14.1 mL vs. 55.7 ± 11.4 mL, $p < 0.001$) than LAA isolation. LAEF
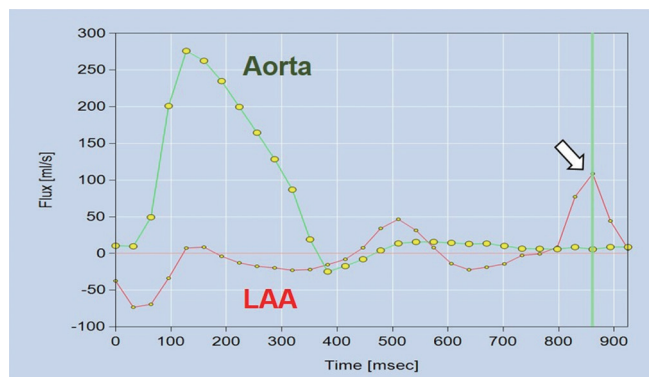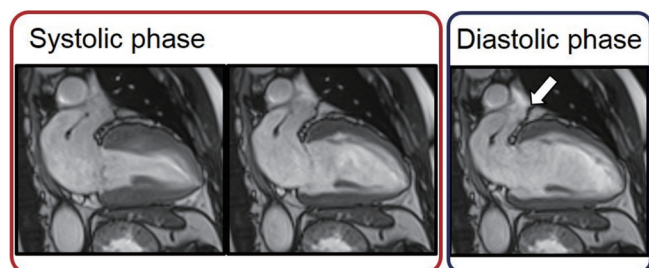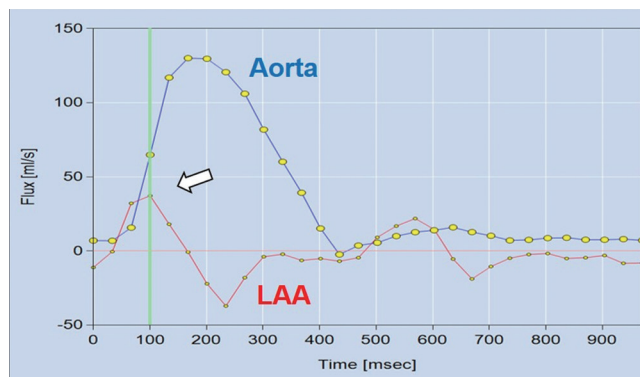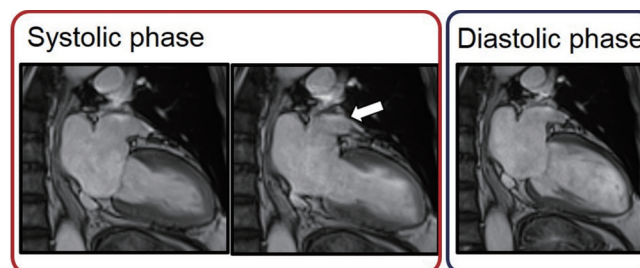
Fig. 4. A 50-year old man without LAA isolation.
The graph **(A)** from VENC-MRI data shows the LAA emptying (arrow) in the late DP. Two-chamber view of cine MRI **(B)** shows a remarkable contraction of LAA (arrow) in the DP of the left ventricle.

Fig. 5. A 48-year old man with LAA isolation.
The graph **(A)** from VENC-MRI data shows the LAA emptying (arrow) in the SP. Two-chamber view of cine MRI **(B)** shows a weak contraction of LAA (arrow) in the SP of the left ventricle. SP = systolic phase

was significantly greater in LAA normal activation (31.1% ± 16.6% vs. 23.7% ± 11.2%, $p = 0.04$) than in LAA isolation. Furthermore, LAA isolation showed significantly lower LAA-EF (40.1 ± 16.2 mL/s vs. 80.2 ± 25.1 mL/s, $p < 0.001$) than LAA normal activation. Thus, the incidence of weak LAA emptying was also significantly greater in LAA isolation (11/23 [48%] vs. 1/61 [2%], $p < 0.001$) than in LAA normal activation. The incidence of LAA emptying in SP was significantly greater in LAA isolation (21/23 [91%] vs. 0/61 [0%], $p < 0.001$) than in LAA normal activation. In comparison to LA-LGE, LAA isolation showed a significantly greater extent of LA-LGE (71.0% ± 19.4% vs. 53.4% ± 19.9%, $p < 0.001$) than LAA normal activation. The incidence of severe LA-LGE was also significantly greater in LAA isolation (18/23 [78%] vs. 28/61 [46%], $p = 0.02$) than in LAA normal activation.

The relationship between LAA-EF and LAV was evaluated in each LAA isolation and normal activation (Fig. 6). In LAA isolation, LAA-EF showed significant positive relationship to LAVmax (R = 0.5, $p = 0.02$) and LAVmin (R = 0.44, $p = 0.04$). In LAA normal activation, LAA-EF showed significant negative relationship to LAVmax (R = -0.27, $p = 0.03$) and LAVmin (R = -0.3, $p = 0.01$).

To identify the independent determinants of LA function after catheter ablation (Table 4), univariate regression analysis showed that there was a significant association between the LAEF and LAA-EF ($p < 0.001$) and LAA-EP ($p = 0.01$), respectively. A multiple linear regression was calculated to predict LAEF and a significant regression equation was found (F [1, 82] = 5.67, $p = 0.01$) with an R^2 of 0.06. Predicted LAEF (in %) was equal to 31.3 - 9.1 x LAA-EP, where the LAA-EP was coded as 0 = in DP and 1 = in SP. LAA emptying in SP decreased LAEF by -9.1% when compared to that in DP. Therefore, LAA-EP was a significant predictor of LAEF.

DISCUSSION

We assessed the LAA emptying and LA function through cardiac MRI among patients who underwent successful catheter ablation of AF and compared them between LAA isolation and normal activation of LAA. Patients without LAA isolation showed significantly lower LAVmax and LAVmin than those with LAA isolation. LAA isolation showed a weak LAA emptying and commonly developed LAA emptying in the SP even with sinus rhythm. LAA emptying

Table 1. Clinical Characteristics of Study Cohort

Characteristics	All (n = 84)	LAA Normal Activation (n = 61)	LAA Isolation (n = 23)	P
Mean age (years)	59 ± 10	59 ± 10	60 ± 12	0.49
Male	67 (80)	46 (75)	21 (91)	0.11
Body surface area (m^2)	1.7 ± 0.1	1.7 ± 0.1	1.8 ± 0.1	0.17
Hypertension	21 (25)	13 (21)	8 (35)	0.21
Diabetes mellitus	5 (6)	3 (5)	2 (9)	0.51
PAF:PeAF	47:37	39:22	8:15	0.01*
LV ejection fraction (%)	55 ± 5	55 ± 5	54 ± 4	0.18

Data are numbers of patients with percentages in parentheses or mean ± SD. *Indicates statistical significance. LV = left ventricular, PAF = paroxysmal atrial fibrillation, PeAF = persistent atrial fibrillation

Table 2. Inter- and Intraobserver Reproducibility in Cardiac MRI Measurements

Cardiac MRI Measurements	Interobserver Reproducibility	Intraobserver Reproducibility
Intraclass correlation coefficient		
LAVmin	0.74	0.71
LAVmax	0.73	0.78
LAA-EF	0.81	0.87
The extent of LA-LGE	0.82	0.83
K statistics		
Weak LAA emptying	0.74	0.68
LAA-EP	0.79	0.71

LAA = left atrial appendage, LAA-EF = LAA emptying flux, LAA-EP = LAA emptying phase, LA-LGE = left atrial late gadolinium enhancement, LAV = left atrial volume, LAVmax = maximum LAV, LAVmin = minimum LAV

in SP showed a significant and positive relationship between the LAA-EF and LAV. In contrast, LAA emptying in DP showed a significant and negative relationship between LAA-EF and LAV, respectively. Finally, LAA emptying was an independent factor to LA function in patients who maintained sinus rhythm after catheter ablation of AF.

AF can lead to reversible chamber dilatation and dysfunction of LA with the extent of rate-related cardiomyopathy (1). Shrinkage of the large LA chamber may occur in patients who undergo catheter ablation of AF, and it has been defined as a reverse remodeling of left atrium (19, 20). This remodeling may be due to the decreased burden of AF and scar formation from the catheter ablation (20). The degree of LA shrinkage strongly correlates with the extent of ablation-induced scarring in the LA wall after catheter ablation of AF. However, in this study, despite the high extent of LA-LGE, patients with LAA isolation had significantly greater LAV after catheter ablation than those without LAA isolation. Furthermore, LAEF after catheter ablation was significantly affected by the LAA hemodynamics after LAA isolation rather than the extent of

LA-LGE. These findings suggest that follow-up after catheter ablation may need a comprehensive evaluation of LAA and left atrium.

Recent catheter ablation strategies include electrical LAA isolation. It has shown promising outcomes in the management of drug-refractory AF (2, 8). However, recent studies have reported an increased stroke risk following LAA isolation (2, 21). Weak LAA emptying after LAA isolation may result in LAA blood stasis, which is associated with the formation of LAA thrombus (2, 9). Thus, patients with LAA isolation should be on long-term oral anticoagulants or considered for LAA occlusion (2). In this study, 48% of patients with LAA isolation showed weak LAA emptying (LAA-EF of < 35 mL/s) even in patients with sinus rhythm. The active use of catheter ablation including LAA isolation will require follow-up evaluation of LA function and LAA hemodynamics in the management of patients who underwent catheter ablation of AF.

LAA acts as a reservoir when the left atrium dilates and left ventricle contracts in the cardiac SP (4, 6). Generally, LAA emptying represents a strong blood flow from the LAA to LA chamber in the DP of the left ventricle (4, 6). Based on the study results, a significant negative relationship was found between LAA-EF and LAV when LAA emptying developed during DP. This can suggest that LAA, as a reservoir, can share the increased preload volume to the LA chamber in the process of LA reverse remodeling following catheter ablation. Interestingly, LAA isolation by catheter ablation alters LAA-EP from DP to SP (21). In this study, LAA emptying in SP showed a significant positive relationship between LAA-EF and LAV. Depending on the LAA-EP, LAA-EF may be considered as an LAA reservoir function or a preload volume factor in the reverse remodeling of LA following the catheter ablation of AF. Furthermore, LAA-EP was an independent factor to LAEF after catheter ablation of AF.

Table 3. Comparison of Cardiac MRI Measurements between the Normal Activation and LAA Isolation

Characteristics	All (n = 84)	LAA Normal Activation (n = 61)	LAA Isolation (n = 23)	P
LAVmin (mL)	33.2 ± 13.0	29.7 ± 12.0	43.3 ± 10.7	< 0.001*
LAVmax (mL)	46.8 ± 14.4	43.8 ± 14.1	55.7 ± 11.4	< 0.001*
LAEF (%)	29.1 ± 15.6	31.1 ± 16.6	23.7 ± 11.2	0.04*
LAA-EF (mL/s)	69.2 ± 29.1	80.2 ± 25.1	40.1 ± 16.2	< 0.001*
Weak LAA emptying	12/84 (14)	1/61 (2)	11/23 (48)	< 0.001*
LAA emptying in SP	21/84 (25)	0/61 (0)	21/23 (91)	< 0.001*
Extent of LA-LGE (%)	58.2 ± 21.2	53.4 ± 19.9	71.0 ± 19.4	< 0.001*
Mild LA-LGE	4/84 (5)	4/61 (7)	0/23 (0)	
Moderate LA-LGE	34/84 (41)	29/61 (47)	5/23 (22)	0.02*
Severe LA-LGE	46/84 (55)	28/61 (46)	18/23 (78)	

Data are numbers of patients with percentages in parentheses or mean ± SD. *Indicates statistical significance. LAEF = left atrial ejection fraction, SP = systolic phase
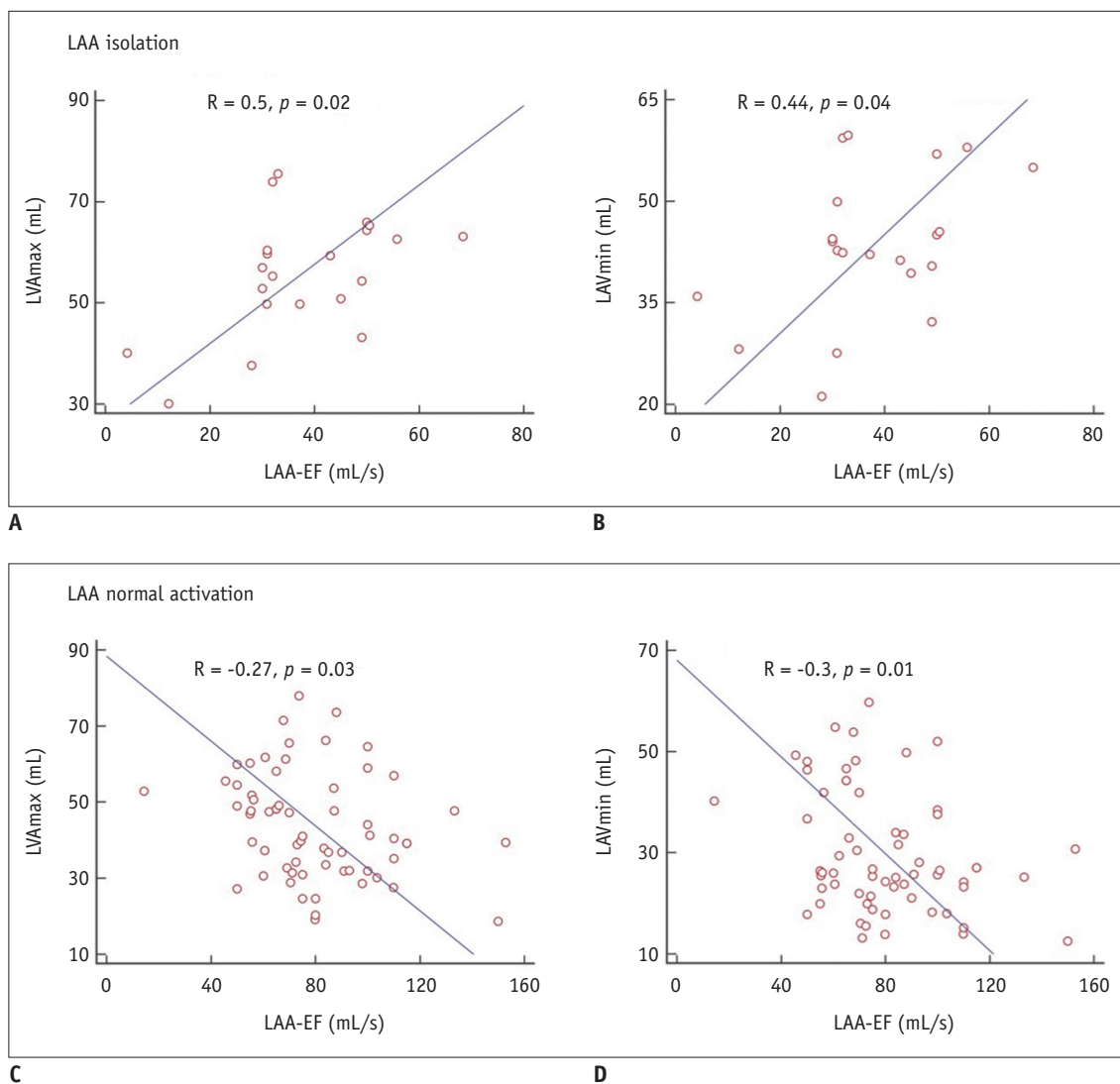

Fig. 6. Relationship between the LAA emptying flux and LAV.
The graphs show the relationships between the LAA-EF, LAVmax, and LAVmin for each LAA isolation **(A, B)** and LAA normal activation **(C, D)**.
LAA-EF = LAA emptying flux, LAVmax = maximum LAV, LAVmin = minimum LAV

Table 4. Independent Determinants of LAEF

Characteristics	Univariate Regression Analysis		Multiple Linear Regression Analysis	
	Coefficient	P	Coefficient	P
Age	0.02	0.88		
Sex (female vs. male)	0.24	0.95		
Hypertension	2.02	0.61		
Diabetes mellitus	-7.43	0.31		
AF type (PAF vs. PeAF)	-2.99	0.38		
LAA normal activation vs. LAA isolation	-9.13	0.05		
Extent of LA-LGE	0.08	0.33		
LAA-EF	0.13	< 0.001*		
LAA-EP (in DP vs. in SP)	-9.13	0.01*	-9.13	0.01*

*Indicates statistical significance. DP = diastolic phase

Some limitations of this study must be addressed. First, our analysis was a retrospective study based on cardiac MRI, and a selective bias may exist. Second, there is no comparison with the baseline LAV and LAA emptying before catheter ablation since the heart rhythm of AF itself might affect the cardiac MRI measurements. Third, validation of the LAA emptying by comparing transesophageal echocardiography may be required. However, transesophageal echocardiography may render patients uncomfortable during examination. Finally, this study requires further clinical studies with more data to define the exact nature of the LAA emptying after catheter ablation and assess its clinical significance such as embolic stroke and recurrent AF.

In conclusion, the typical cardiac MRI feature of LAA isolation was LAA emptying in SP even with sinus rhythm after catheter ablation of AF. Furthermore, the LAA emptying in SP may be associated with a loss of LAA reservoir function and a decrease in LAEF in patients who maintain sinus rhythm after successful catheter ablation of AF.

Conflicts of Interest

The authors have no potential conflicts of interest to disclose.

ORCID iDs

Jaemin Shim
  https://orcid.org/0000-0001-8251-1522
Jong-il Choi
  https://orcid.org/0000-0001-6617-508X
Young-Hoon Kim
  https://orcid.org/0000-0002-4254-647X
Sung Ho Hwang
  https://orcid.org/0000-0003-1850-0751

REFERENCES

1. Kirchhof P, Benussi S, Kotecha D, Ahlsson A, Atar D, Casadei B, et al. 2016 ESC guidelines for the management of atrial fibrillation developed in collaboration with EACTS. *Eur J Cardiothorac Surg* 2016;50:e1-e88
2. Calkins H, Hindricks G, Cappato R, Kim YH, Saad EB, Aguinaga L, et al. 2017 HRS/EHRA/ECAS/APHRS/SOLAECE expert consensus statement on catheter and surgical ablation of atrial fibrillation. *Heart Rhythm* 2017;14:e275-e444
3. Reddy VY, Sievert H, Halperin J, Doshi SK, Buchbinder M, Neuzil P, et al. Percutaneous left atrial appendage closure vs warfarin for atrial fibrillation: a randomized clinical trial. *JAMA* 2014;312:1988-1998
4. Naksuk N, Padmanabhan D, Yogeswaran V, Asirvatham SJ. Left atrial appendage: embryology, anatomy, physiology, arrhythmia and therapeutic intervention. *JACC Clin Electrophysiol* 2016;2:403-412
5. Romero J, Cao JJ, Garcia MJ, Taub CC. Cardiac imaging for assessment of left atrial appendage stasis and thrombosis. *Nat Rev Cardiol* 2014;11:470-480
6. Hwang SH, Roh SY, Shim J, Choi JI, Kim YH, Oh YW. Atrial fibrillation: relationship between left atrial pressure and left atrial appendage emptying determined with velocity-encoded cardiac MR imaging. *Radiology* 2017;284:381-389
7. Ohara K, Hirai T, Fukuda N, Sakurai K, Nakagawa K, Nozawa T, et al. Relation of left atrial blood stasis to clinical risk factors in atrial fibrillation. *Int J Cardiol* 2009;132:210-215
8. Di Biase L, Burkhardt JD, Mohanty P, Sanchez J, Mohanty S, Horton R, et al. Left atrial appendage: an underrecognized trigger site of atrial fibrillation. *Circulation* 2010;122:109-118
9. Rillig A, Tilz RR, Lin T, Fink T, Heeger CH, Arya A, et al. Unexpectedly high incidence of stroke and left atrial appendage thrombus formation after electrical isolation of the left atrial appendage for the treatment of atrial tachyarrhythmias. *Circ Arrhythm Electrophysiol* 2016;9:e003461
10. Chavhan GB, Babyn PS, Jankharia BG, Cheng HL, Shroff MM. Steady-state MR imaging sequences: physics, classification,

and clinical applications. *RadioGraphics* 2008;28:1147-1160

11. Caudron J, Fares J, Bauer F, Dacher JN. Evaluation of left ventricular diastolic function with cardiac MR imaging. *Radiographics* 2011;31:239-259

12. Muellerleile K, Sultan A, Groth M, Steven D, Hoffmann B, Adam G, et al. Velocity encoded cardiovascular magnetic resonance to assess left atrial appendage emptying. *J Cardiovasc Magn Reson* 2012;14:39

13. Lee HG, Shim J, Choi JI, Kim YH, Oh YW, Hwang SH. Use of cardiac computed tomography and magnetic resonance imaging in case management of atrial fibrillation with catheter ablation. *Korean J Radiol* 2019;20:695-708

14. Lee JW, Hur JH, Yang DH, Lee BY, Im DJ, Hong SJ, et al. Guidelines for cardiovascular magnetic resonance imaging from the Korean society of cardiovascular imaging-part 2: interpretation of cine, flow, and angiography data. *Korean J Radiol* 2019;20:1477-1490

15. Hwang SH, Oh YW, Kim MN, Park SM, Shim WJ, Shim J, et al. Relationship between left atrial appendage emptying and left atrial function using cardiac magnetic resonance in patients with atrial fibrillation: comparison with transesophageal echocardiography. *Int J Cardiovasc Imaging* 2016;32:163-171

16. Lee DK, Shim J, Choi JI, Kim YH, Oh YW, Hwang SH. Left atrial fibrosis assessed with cardiac MRI in patients with paroxysmal and those with persistent atrial fibrillation. *Radiology* 2019;292:575-582

17. Shrout PE, Fleiss JL. Intraclass correlations: uses in assessing rater reliability. *Psycho Bull* 1979;86:420-428

18. McHugh ML. Interrater reliability: the kappa statistic. *Biochem Med (Zagreb)* 2012;22:276-282

19. Wylie JV Jr, Peters DC, Essebag V, Manning WJ, Josephson ME, Hauser TH. Left atrial function and scar after catheter ablation of atrial fibrillation. *Heart Rhythm* 2008;5:656-662

20. Kim JS, Im SI, Shin SY, Kang JH, Na JO, Choi CU, et al. Changes in left atrial transport function in patients who maintained sinus rhythm after successful radiofrequency catheter ablation for atrial fibrillation: a 1-year follow-up multislice computed tomography study. *J Cardiovasc Electrophysiol* 2017;28:167-176

21. Kim YG, Shim J, Oh SK, Lee KN, Choi JI, Kim YH. Electrical isolation of the left atrial appendage increases the risk of ischemic stroke and transient ischemic attack regardless of postisolation flow velocity. *Heart Rhythm* 2018;15:1746-1753